ANNUAL REVIEWS

*Annual Review of Earth and Planetary Sciences*

# The Impact of Volcanic Eruptions on Tropical Hydroclimate

Roberta D'Agostino,[1] Shih-Wei Fang,[2] Myriam Khodri,[3] Francesco S.R. Pausata,[4] Ernesto Tejedor,[5] Claudia Timmreck,[6] and Davide Zanchettin[7,8]

[1]Institute of Atmospheric Sciences and Climate, National Research Council, Lecce, Italy; email: roberta.dagostino@cnr.it

[2]Department of Atmospheric Sciences, National Central University, Taoyuan, Taiwan

[3]Laboratoire d'Océanographie et du Climat: Expérimentations et Approches Numériques/ Institut Pierre-Simon Laplace, Sorbonne Université/IRD/CNRS/MNHN, Paris, France

[4]Center for the Study and Simulation of Climate at Regional Scale and Research Center on the Dynamics of the Earth System, Department of Earth and Atmospheric Sciences, University of Quebec at Montreal, Montreal, Quebec, Canada

[5]Department of Geology, National Museum of Natural Sciences, Spanish National Research Council, Madrid, Spain

[6]Max Planck Institute for Meteorology, Hamburg, Germany

[7]Department of Environmental Sciences, Informatics and Statistics, Ca'Foscari University of Venice, Mestre, Italy

[8]Istituto Nazionale di Geofisica e Vulcanologia, Catania, Italy



Annu. Rev. Earth Planet. Sci. 2026. 54:365–87

First published as a Review in Advance on January 28, 2026

The *Annual Review of Earth and Planetary Sciences* is online at earth.annualreviews.org

https://doi.org/10.1146/annurev-earth-071025-112048



## Keywords

volcanic forcing, tropical hydroclimate, energy framework, ENSO, modeling, reconstructions

## Abstract

Volcanic eruptions exert a profound influence on tropical hydroclimate, including interannual variability associated with the El Niño–Southern Oscillation. This review synthesizes recent advances in understanding these impacts through an energy framework that links radiative forcing to shifts in the Intertropical Convergence Zone (ITCZ) and global monsoon systems. While global responses are robust in climate models, regional expressions remain uncertain due to biases and limitations in both simulations and paleoclimate reconstructions. Nonetheless, consistent patterns emerge—such as ITCZ displacement and reduced monsoon precipitation—that align with energetic theory, offering a physically grounded explanation for observed hydroclimatic anomalies following eruptions. This framework also provides a basis for estimating potential hydroclimate impacts of future volcanic events.

- Volcanic eruptions strongly influence tropical hydroclimate, but the mechanisms linking radiative forcing to large-scale responses are not fully understood.
- We assess evidence from climate models and paleoclimate reconstructions, noting robust global responses but regional differences due to model biases and data limitations.
- The energy framework provides a physically based foundation for anticipating tropical hydroclimate responses to future volcanic eruptions.
- Consistent patterns emerge such as ITCZ shifts and weakened monsoons, explained by energy theory and underpinned by observed posteruption climate anomalies.



## 1. INTRODUCTION

Strong explosive volcanic eruptions temporarily enhance the stratospheric sulfate aerosol layer, which is a major natural driver of climate variability. This enhanced aerosol layer increases planetary albedo, leading to global surface cooling, suppression of the hydrological cycle, and potentially severe ecological and societal impacts (see overview articles Timmreck 2012, Marshall et al. 2022, Büntgen et al. 2026). However, quantification of these responses remains poorly constrained in spite of decades of scientific research (e.g., Zanchettin et al. 2022), with increasing uncertainties for regional responses (e.g., Marshall et al. 2022, Villamayor et al. 2023). These knowledge gaps reflect the complexity of aerosol–climate interactions and the dynamics underlying climate responses. This complexity is compounded by the limited number of observed events available for characterization, model validation, and hypothesis testing.

The 1991 eruption of Mt. Pinatubo remains the paradigm for studying volcanic impacts on climate, as it is the best-observed event in the historical record (e.g., Kremser et al. 2016). It provides a crucial reference for numerical experiments investigating uncertainties in volcanic forcing (e.g., Quaglia et al. 2023), for evaluating climate impacts of eruptions and their predictability (e.g., Zanchettin et al. 2022, Bilbao et al. 2024), and for calibrating reconstructions of volcanic forcing (e.g., Toohey et al. 2016, Aubry et al. 2025). Studying earlier eruptions—similar in size or larger than Pinatubo but less well-constrained—has become crucial for understanding the wider range of volcanic impacts on climate beyond the specifics of the Pinatubo event (e.g., Zanchettin et al. 2016).

For near-surface air temperature, large networks of instrumental temperature measurements stretch back into the nineteenth century and encompass several additional large volcanic eruptions. Global cooling robustly emerges as a typical response to volcanic forcing (see, e.g., Marotzke & Forster 2015, Eyring et al. 2021), notwithstanding eruption specificities regarding magnitude, location, timing, and background climate conditions. Instrumental observations covering the 1809 unidentified event and the 1815 Mount Tambora eruption indicate the potential of strong volcanic clusters to produce global cooling on decadal timescales (e.g., Brönnimann et al. 2019). Instrumental data, together with proxy reconstructions and documentary evidence, reveal recurring regional patterns in posteruption temperature anomalies, most notably equatorial Pacific warming resembling a positive El Niño phase (e.g., McGregor et al. 2020, Dogar et al. 2023). However, studies also reveal inconsistencies between observations, reconstructions, and simulations, which challenges the idea of well-constrained expected regional responses to volcanic forcing (e.g., Zanchettin et al. 2015, Timmreck et al. 2021).

The dynamical interpretation of global and regional posteruption temperature anomalies is supported by an increasing number of climate model experiments. These range from realistic historical full-forcing simulations to idealized volcanic forcing and mechanistic experiments, carried out with numerical models of varying complexity. Recently, the increasing use of multi-model and large ensemble approaches has underlined the critical dependency of the temperature response on initial conditions. For instance, climate models yield a too-strong expected posteruption cooling compared to observations (e.g., Chylek et al. 2020), but this is partly explained by sampling biases of initial conditions, primarily related to the El Niño–Southern Oscillation (ENSO) phase (e.g., Lehner et al. 2016). Modes of climate variability therefore not only contribute to determining expected dynamical responses but also can significantly affect statistics of posteruption temperature anomalies (e.g., Zanchettin et al. 2022).

Volcanic effects on the hydrological cycle are less understood than temperature responses. A robust decrease in global and tropical mean precipitation has been detected within a few years after major volcanic eruptions (e.g., Trenberth & Dai 2007; Iles & Hegerl 2014, 2015). Despite this, in principle agreeing with a slowdown of the hydrological cycle under global cooling, regional patterns indicate that the global response stems from drying of climatologically wet regions while climatologically dry regions become wetter (e.g., Iles & Hegerl 2014, Zuo et al. 2019b). This response pattern is opposite to what is expected under global warming (e.g., Iles et al. 2013, Schurer et al. 2020).

The Sixth Assessment Report of the Intergovernmental Panel on Climate Change (Douville et al. 2021) expresses high confidence in posteruption precipitation declines in tropical wet regions but also notes low confidence in the regional and seasonal characteristics of volcanic impacts on precipitation in the tropics. Low confidence stems from the scarcity and noisiness of precipitation observations providing for a low signal-to-noise ratio on volcanic fingerprints (Hegerl et al. 2015). Further uncertainty arises from the inherent complexity of the tropical hydrological cycle: Rainfall patterns depend on monsoons and the position of the Intertropical Convergence Zone (ITCZ), and their response is not always consistent across different regions, as it depends on the forcing characteristics. Additionally, observational studies have mostly looked at specific areas rather than the whole tropics. For example, records show that large eruptions often lead to weaker summer monsoons (e.g., Joseph & Zeng 2011): In India, rainfall was reduced for up to two years after major eruptions in the nineteenth and twentieth centuries (e.g., Fadnavis et al. 2021). In the Sahel, severe droughts have been more likely after large Northern Hemisphere (NH) eruptions, which may be linked to the ITCZ shifting toward the warmer hemisphere (Haywood et al. 2013). These findings highlight the response of regional rainfall patterns, but they do not yet provide a clear, consistent picture for the whole tropics—something this review aims to address.

From a climate modeling perspective, the tropics are a key region where inconsistencies in posteruption climate and especially hydroclimate variability are found across different models (e.g., Tejedor et al. 2021a, Zanchettin et al. 2022). Current climate models suffer from similar limitations as previous generation models regarding the simulation of tropical precipitation, which is invoked to explain the enduring bias in the response to volcanic forcing, seen as an overly strong reduction of precipitation (Fiedler et al. 2020). Beyond forcing, much of the uncertainty arises from the dynamics and thermodynamics of tropical systems. Key factors include major circulation patterns (monsoons, Hadley and Walker circulations), climate modes such as ENSO, and feedbacks such as lapse-rate feedback, cloud feedbacks, and moisture–convection feedback.

This literature review synthesizes and discusses recent advances in the knowledge and understanding of volcanically forced tropical hydroclimate variability. It integrates results from instrumental records, proxy reconstructions, climate modeling, and theories based on an energy framework. We primarily focus on literature published since 2015, reflecting the significant methodological and conceptual developments in the field over the last decade.

**ENSO:** a natural climate pattern of warming and cooling in the tropical Pacific Ocean that disrupts global weather, shifting rainfall, storms, and temperatures every few years

**Hadley and Walker circulations:** large-scale convective motions in the tropics; the Hadley moves air north–south between the equator and subtropics, while the Walker moves air east–west across the Pacific, together shaping rainfall and climate around the tropics

**Lapse-rate feedback:** climate feedback that arises because warming alters the vertical temperature gradient of the atmosphere, which enhances outgoing radiation to space and thus weakens the overall greenhouse effect

**Cloud feedbacks:** the processes by which changes in clouds, induced by climate forcing (such as greenhouse gas increases and volcanic emissions), act to either amplify (positive feedback) or dampen (negative feedback) the overall climate response

**Moisture–convection feedback:** climate process where a warmer atmosphere holds more water vapor, enhancing convective instability and leading to stronger precipitation and latent heat release, which can further amplify atmospheric circulation and sustain convection

Our focus is placed on the understanding of the underlying fundamental physical processes and mechanisms, with the aim of disentangling the complexity arising from interactions between radiation, large-scale circulation of the ocean and atmosphere, feedbacks, and local processes. We specifically concentrate on a core set of physical processes, including ITCZ shifts, and monsoon modulation, and we explore how different data sources and methods contribute to our understanding of volcanically forced tropical hydroclimate variability over the Common Era.

This review is structured as follows. In Section 2, we introduce the theoretical argument we use for interpreting hydroclimate response to volcanic forcing, i.e., an energy framework that connects energy budget anomalies to tropical atmospheric overturning and precipitation changes. In Section 3, we characterize reconstructed volcanically forced tropical hydroclimate variability over the last millennium from available proxy-based datasets. Section 4 focuses on recent advances on the volcanic impact of tropical hydroclimate with modeling studies. Section 5 concludes the review with an outlook on future implications.

## 2. AN ENERGY FRAMEWORK FOR UNDERSTANDING TROPICAL PRECIPITATION AND ATMOSPHERIC CIRCULATION RESPONSE TO VOLCANIC ERUPTIONS

Scanning through recent literature (Colose et al. 2016, Erez & Adam 2021, D'Agostino & Timmreck 2022), we see that the response of the tropical hydroclimate to volcanic eruptions has often been interpreted through the moist static energy (MSE) framework. First introduced by Neelin & Held (1987), it provides a theoretical basis for predicting tropical precipitation changes under external forcings. This framework has been widely used to analyze hydroclimatic responses to global warming, Atlantic Meridional Overturning Circulation slowdown, orbital forcing, and volcanic eruptions—particularly those introducing large interhemispheric energy asymmetries (Kang et al. 2008, 2009; Marshall et al. 2014; Lionello et al. 2024; McGraw & Polvani 2024).

In brief, model simulations indicate that large tropical volcanic eruptions induce tropospheric cooling, particularly over land, leading to cloud suppression, weakened deep convection, and weaker updrafts in the Hadley cell (HC). These changes are accompanied by an equatorward contraction of the ITCZ and have been shown to affect tropical regions for up to two summers after the eruption. Proxy reconstructions and model simulations over the last millennium provide further evidence for these hydroclimatic responses (e.g., Ridley et al. 2015, Colose et al. 2016, Alfaro-Sánchez et al. 2018).

When a volcanic eruption creates an energy imbalance between the NH and the Southern Hemisphere (SH), the tropical rain belt and the ITCZ tend to shift toward the hemisphere that is relatively warmer and receives more energy (i.e., the one less affected by the eruption). This means that rainfall patterns can change across large parts of the tropics depending on where the imbalance occurs.

In this section we show the basics of the energy framework and MSE budget (Section 2.1), and we describe the response of the tropical overturning and thermodynamics and dynamics according to the theoretical expectations in Sections 2.2 and 2.3, respectively.

### 2.1. Energy Framework and Moist Static Energy Budget

The central idea of the energy framework is that the net import of MSE into the atmospheric column—balanced by latent heating associated with precipitation—determines the spatial distribution of tropical rainfall. In the steady-state approximation, the vertically integrated atmospheric energy budget is

$$\langle \nabla(\bar{u}h) \rangle \approx NEI = R_{\mathrm{TOA}} - F_{\mathrm{sfc}}, \tag{1}$$

where $\langle \nabla(\bar{u}h) \rangle$ is the divergence of the vertically integrated total MSE flux, NEI is the net energy input, $R_{\mathrm{TOA}}$ is the net radiative flux at the top of the atmosphere, and $F_{\mathrm{sfc}}$ is the net surface flux. MSE is defined as

$$h = c_p T + L_v q + gz, \tag{2}$$

where $c_p T$ is sensible heat, $L_v q$ is latent heat, and $gz$ is potential energy. MSE is conserved in moist adiabatic processes and serves as a tracer of large-scale energy transport. Regions of net MSE convergence coincide with strong precipitation, while divergence characterizes dry zones. The assumption of steady state makes the atmospheric storage term small under seasonal and other long-term means (e.g., annual, interannual) (Adam et al. 2016).

In the zonal mean ([·]), Equation 1 becomes

$$\partial_y \langle [vh] \rangle \approx NEI. \tag{3}$$

In local Cartesian coordinates, the spatial derivatives can be expressed as the meridional distance: $y = a\phi$, where $a$ is Earth's radius and $\phi$ denotes latitude.

By expanding the zonally averaged MSE flux around the equator (Equation 3) to first order in latitude, and assuming it is zero at the ITCZ, one obtains the following (Bischoff & Schneider 2014):

$$ITCZ_\phi \approx -\frac{1}{a}\frac{\langle [vh]_0 \rangle}{\partial_y \langle [vh]_0 \rangle} \approx \frac{AET_0}{NEI_0}, \tag{4}$$

where $a$ is Earth's radius and AET is the atmospheric energy transport—the vertically integrated meridional MSE flux at the equator. Subscript 0 indicates area-weighted average along equatorial values: specifically, between 5°N and 5°S for AET and 10°N and 10°S for NEI.

The energy flux equator (EFE)—the latitude where AET energy balances out to zero—is particularly informative. When AET is directed northward, the ITCZ shifts southward, and vice versa.

Volcanic aerosols perturb the top-of-atmosphere energy balance by scattering incoming solar radiation, reducing surface heating, and inducing asymmetric cooling across hemispheres. The magnitude of this asymmetry depends on eruption location and season (see **Figure 1**) and could be summarized as shown in the sidebar titled Eruption-Latitude-Specific Responses.

In all cases, the direction and magnitude of ITCZ migration correspond to the energy flux adjustments required to balance hemispheric radiative anomalies.

**Net surface flux:** the sum of energy exchanges between Earth's surface and the atmosphere, including absorbed and emitted radiation, turbulent fluxes of sensible heat (from temperature differences), and latent heat (from evaporation and condensation), as well as small contributions from conduction

**Moist adiabatic processes:** thermodynamic processes in which a saturated air parcel ascends or descends without exchange of heat with its environment, such that expansion or compression occurs adiabatically while condensation or evaporation of water vapor takes place within the air parcel

## 2.2. Atmospheric Energy Transport, Hadley Circulation, and Tropical Precipitation

Volcanic eruptions alter the whole tropical circulation, including the ITCZ and HC. The MSE framework links these changes in overturning circulation to precipitation anomalies via energy flux (Geen et al. 2020). When aerosol-induced surface cooling is greater over land than over ocean—as often occurs following NH eruptions—the land–ocean MSE gradient weakens, reducing monsoon inflow and suppressing precipitation. Being a thermally direct circulation that transports moisture and energy away from the equator, the HC responds sensitively to volcanic forcing, particularly in the years immediately following large eruptions (Erez & Adam 2021, D'Agostino & Timmreck 2022). NH eruptions are typically followed by drying across the NH monsoons (i.e., Indian, West

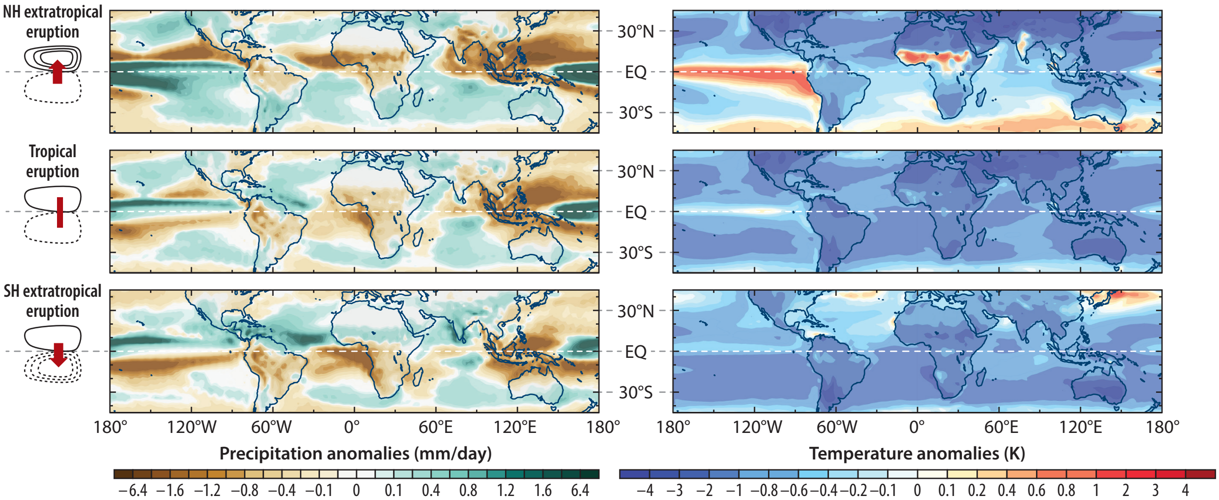


**Figure 1**

Hydroclimate response to NH extratropical, tropical, and SH extratropical eruptions (*top*, *middle*, and *bottom rows*, respectively) from the Max Planck Institute Grand Ensemble EVA-ENS experiment (Azoulay et al. 2021, Timmreck et al. 2024). Ensemble mean 1992 (i.e., the first year after an eruption imposed in June 1991) precipitation anomalies in mm/day are shown in brown-to-green colors, and temperature anomalies are shown in blue-to-red colors. Anomalies are computed as the difference between the experiment with the strongest emission (40 TgS) and the control run without volcanic forcing. All values shown are statistically significant among the 100-member ensemble. On the left side of the figure are sketches of anomalous Hadley circulation: Northern circulation is the solid line, and the southern counterpart is the dashed line. Fewer/more isolines of the meridional mass stream function indicate a weaker/stronger circulation. Red arrows indicate the anomalous AET, toward the cooler hemisphere. In the tropical eruption case, anomalous AET is invariant. Abbreviations: AET, atmospheric energy transport; EVA-ENS, Easy Volcanic Aerosol ensemble; NH, Northern Hemisphere; SH, Southern Hemisphere.

African, North American) and enhanced rainfall in SH regions (i.e., South America and South Africa). In response to asymmetric volcanic forcing, anomalous AET is directed toward the preferentially forced hemisphere, along the imposed temperature gradient. The equatorial AET for NH (SH) eruption is northward (southward), but the ITCZ position is negatively correlated to AET (Erez & Adam 2021). As a result, the HC is stronger in the cooler hemisphere with NEI deficit

## ERUPTION-LATITUDE-SPECIFIC RESPONSES

1. NH extratropical eruptions (e.g., Laki 1783, Katmai 1912) preferentially cool the NH, resulting in a south-to-north AET and a southward ITCZ shift. This weakens NH monsoons and enhances SH monsoons.
2. SH extratropical eruptions (e.g., Kuwae 1458) generate the opposite effect, shifting the ITCZ northward and strengthening/weakening NH/SH monsoons.
3. Tropical eruptions (e.g., Tambora 1815, Pinatubo 1991) tend to produce hemispherically symmetric cooling but still elicit asymmetric responses due to differences in background climate, aerosol dispersion patterns, and land distribution. These events often weaken global monsoon strength without strong ITCZ displacement. It should be noted that some tropical eruptions have a strong asymmetric aerosol load. For example, in the 1963 Agung eruption, the volcanic cloud was predominantly located in the SH, and in the 1984 El Chichón eruption, the volcanic cloud was predominantly located in the NH. The response to these eruptions is more comparable to that of extratropical eruptions.

and weaker in the warmer hemisphere with NEI gain. Tropical eruptions result in more symmetric changes: Monsoons decline in both hemispheres, and the HC is weaker and narrower (Erez & Adam 2021, D'Agostino & Timmreck 2022). These changes are well-represented in climate models with idealized NH and SH extratropical eruptions and tropical eruptions (**Figure 1**). High-resolution model simulations (e.g., the Geophysical Fluid Dynamics Laboratory High-Resolution Atmosphere Model (HiRAM) Atmospheric Model Intercomparison Project at 50- and 25-km horizontal resolution) and reanalysis datasets show that eruptions such as El Chichón (1982) and Pinatubo (1991) led to HC weakening and equatorward contraction of its ascending branch. These shifts were accompanied by equatorward displacement of subtropical jets and changes in the thermal contrast between the stratosphere and troposphere (Dogar 2018). The more poleward latitude of El Chichón (17°N) compared to Pinatubo (15°N) led to a stronger hemispheric asymmetry and a more pronounced ITCZ shift. On longer timescales, sequences of large eruptions—such as those linked to the onset of the Little Ice Age—have contributed to persistent global cooling and sustained southward ITCZ displacement (e.g., Winter et al. 2015, Atwood et al. 2020, Steinman et al. 2022). These slow-evolving changes can be interpreted through shifts in the EFE, which migrates toward the hemisphere experiencing greater net radiative input. Moreover, the zonal mean annual ITCZ position being north of the equator implies that ITCZ shifts due to NH versus SH eruptions produce distinct zonal wind stress anomalies. These, in turn, modulate ocean–atmosphere interactions in the Pacific, leading to contrasting ENSO-like responses (Haywood et al. 2013, Atwood et al. 2020) (see Section 4). Later we discuss in detail that the resulting hydroclimatic anomalies are consistent across both paleoclimate reconstructions (Section 3) and model simulations (Section 4).

**Global monsoon:** the aggregation of all regional monsoon systems, reflecting the seasonal reversal of winds and rains across the tropics as a single, interconnected climate pattern

## 2.3. Thermodynamic and Dynamic Mechanisms

Hydroclimate responses to volcanic forcing can be further diagnosed using a moisture budget decomposition, which separates precipitation changes into thermodynamic and dynamic components (Seager et al. 2010; D'Agostino et al. 2019, 2020). The thermodynamic term accounts for changes in specific humidity primarily due to cooling, while the dynamic term includes vertical motion and horizontal moisture convergence anomalies associated with circulation changes (mainly mean flow changes, i.e., the HC in the tropics). Analysis across global monsoon regions shows that dynamic effects dominate the posteruption hydroclimate response (Zuo et al. 2019a). Eruption-induced circulation changes—particularly in the Hadley and Walker circulations—redistribute moisture and modulate precipitation more strongly than changes in atmospheric moisture content alone. After NH extratropical eruptions, the aerosol-induced cooling is strongest over land, diminishing the land–ocean thermal gradient and weakening the MSE contrast. This suppresses monsoon flow and rainfall, and it reduces cross-equatorial energy transport from the SH. The weakened ascent over NH monsoon domains is a key driver of dynamically induced monsoon drying. In contrast, SH extratropical eruptions induce a reversed energy gradient, strengthening NH monsoons while suppressing SH rainfall. These responses illustrate the tight coupling between energy transport direction and atmospheric circulation intensity. Tropical eruptions, despite producing more symmetric global cooling, can still cause regional asymmetries in hydroclimate due to heterogeneous aerosol distribution and preexisting climatological differences. By reducing the land–ocean MSE gradient globally, such eruptions weaken the large-scale overturning circulation, leading to broadly suppressed monsoon precipitation across both hemispheres. Most of the changes within the tropics in the first year after the eruptions are largely dynamical. Overall, precipitation anomalies following volcanic eruptions are consistent with dynamically mediated responses embedded within the energy framework. This approach helps reconcile spatially diverse hydroclimatic outcomes by linking them to large-scale circulation shifts and energy transport requirements.

## 3. ASSESSING HYDROCLIMATE IMPACTS OF LOW-LATITUDE VOLCANIC ERUPTIONS USING TREE-RING AND DATA ASSIMILATION PROXIES

Large tropical volcanic eruptions are among the most significant natural drivers of climate variability over the Common Era. Advances in ice-core synchronization have improved the precision of eruption timing and magnitude estimates (e.g., Toohey & Sigl 2017). At the same time, high-resolution proxy records—including tree-ring width (TRW), maximum latewood density (MXD), and coral $\delta^{18}$O—alongside emerging data assimilation (DA) products have become essential tools for inferring the climate system's sensitivity to volcanic forcing. DA approaches combine proxy records with climate model priors to generate spatially and temporally complete reconstructions of temperature and hydroclimate variables. Key DA products include the Last Millennium Reanalysis (LMR) (Tardif et al. 2019) and the Paleo Hydrodynamics Data Assimilation (PHYDA) (Steiger et al. 2018). Despite methodological differences (e.g., assimilation schemes, priors, temporal resolution), both provide gridded reconstructions of surface climate across the last millennium, allowing assessments of hemispheric and tropical climate responses to volcanic eruptions. In this section, we review and compare the hydroclimatic impacts of large low-latitude volcanic eruptions—with sulfur emissions larger than the 1991 Pinatubo eruption—over the last millennium. Particular emphasis is placed on the hydrodynamic responses within the tropics, where the interactions between volcanic forcing and atmospheric circulation remain complex and uncertain. We explore patterns of agreement and divergence across tree-ring–based drought atlases and DA products, discuss the persistence of posteruption wetting and drying, and assess the potential role of mechanisms such as ITCZ displacement, ENSO modulation, and HC weakening in shaping tropical hydroclimatic variability.

### 3.1. Reconstructed Temperature Responses

Paleoclimate reconstructions consistently show global surface cooling following major tropical eruptions. MXD-based reconstructions, such as the NH stack (Schneider et al. 2015, Stoffel et al. 2015), capture sharp summer cooling peaking within 1–2 years posteruption, with recovery by year five. TRW-based datasets such as N-TREND (Northern Tree-Ring Network Development) (Anchukaitis et al. 2017) depict similar cooling trends but with attenuated amplitudes due to tree biological memory and lower sensitivity to short-term temperature extremes. LMR and PHYDA simulate comparable posteruption cooling (Tejedor et al. 2021b, He et al. 2026), with the strongest signals over land and in NH mid-latitudes. Typical anomalies range from −0.3°C to −0.6°C, aligning well with proxy-only estimates. Spatial differences in cooling reflect variations in proxy coverage and model priors. PHYDA, which assimilates seasonal (e.g., June–August) and annual proxies, has been evaluated seasonally to align with drought atlases such as the North American Drought Atlas (NADA) and the Greater Eurasian Drought Atlas (GEDA) (Cook et al. 2010, 2024). LMR, which assimilates only annually resolved proxies, produces annual mean fields; however, large-scale volcanic signals are broadly consistent across both annual and seasonal reconstructions (Steiger et al. 2018, Tejedor et al. 2021b). In proxy-based products, the cooling after low-latitude eruptions within the tropics is generally weaker than in the NH or in climate simulations (Tejedor et al. 2021b). It remains uncertain whether this weaker signal in the tropics reflects a true climatic response—possibly modulated by oceanic thermal inertia—or is the result of sparser proxy coverage and reduced signal-to-noise ratio in tropical archives.

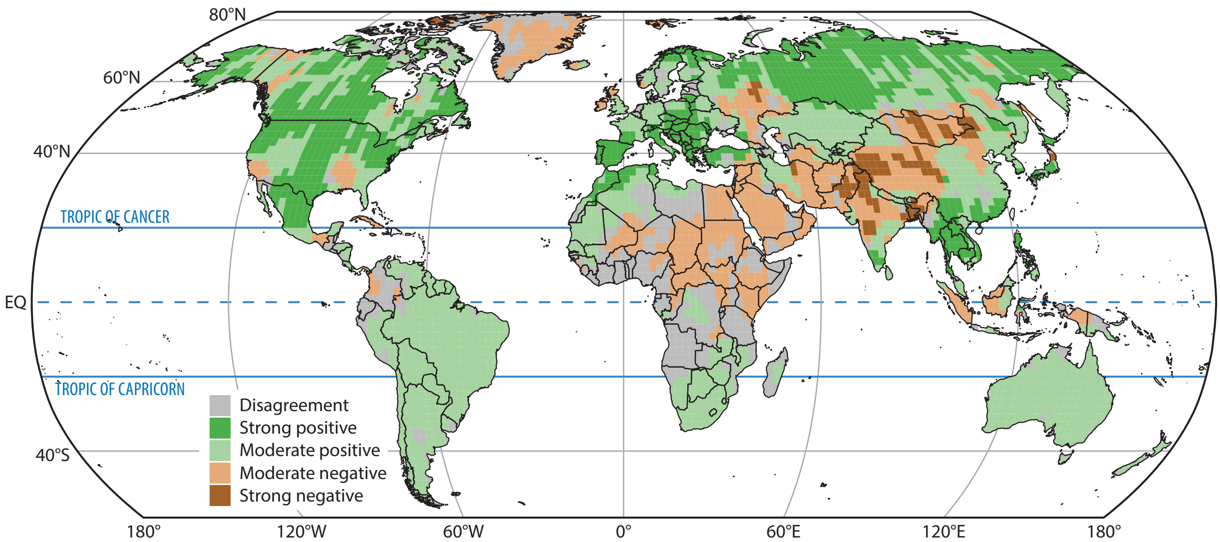


**Figure 2**

Agreement and disagreement in reconstructed PDSI responses during the first three years (years 0 to 3) following 14 large tropical volcanic eruptions over the last millennium [i.e., those with stratospheric sulfate injection exceeding that of Pinatubo in 1991 (Toohey et al. 2019), considering only the later eruption when two occur within 10 years]. The results are based on two drought atlases derived exclusively from tree-ring data—GEDA (Cook et al. 2024) and NADA (Cook et al. 2010)—and two paleoclimate data assimilation products: LMR (Tardif et al. 2019) and PHYDA (Steiger et al. 2018). Agreement is classified as follows: strong positive (*dark green*) or strong negative (*dark brown*) where three out of three overlapping products agree on the sign of PDSI anomalies (wet or dry); moderate positive (*light green*) or moderate negative (*light brown*) where only two out of three reconstructions agree; and disagreement (*gray*) where the signal is inconsistent. The season used for PHYDA is June–August to ensure comparability with the drought atlases; LMR reflects annual mean PDSI. The map highlights areas of robust hydroclimatic response to volcanic forcing, as well as regions with high uncertainty or conflicting signals among reconstructions. Abbreviations: GEDA, Greater Eurasian Drought Atlas; LMR, Last Millennium Reanalysis; NADA, North American Drought Atlas; PDSI, Palmer Drought Severity Index; PHYDA, Paleo Hydrodynamics Data Assimilation.

## 3.2. Hydroclimate Patterns and Regional Agreement

In contrast to the relatively robust temperature response, reconstructed hydroclimatic changes—particularly those reflected in the Palmer Drought Severity Index—are more spatially heterogeneous. Tree-ring–based drought atlases such as NADA and GEDA offer regionally detailed insight into posteruption moisture variability. These reconstructions reveal patterns of wetting in regions such as western North America, the Mediterranean, and southern South America—findings corroborated by DA products and consistent with model simulations (Colose et al. 2016, Stevenson et al. 2016). The convergence across proxy- and DA-based reconstructions supports the physical plausibility of posteruption hydroclimatic responses, often linked to shifts in atmospheric circulation. Enhanced precipitation in the Mediterranean, the western United States, and southern South America aligns with storm track displacement and thermodynamic land–sea contrast (**Figure 2**). These regions of agreement suggest that volcanic signals can override internal variability. Over Eurasia, the forced response appears tied to a negative phase of the East Atlantic Pattern (Rao et al. 2017), which drives spring uplift over the western Mediterranean, southward-shifted storm tracks, and a weakened meridional pressure gradient. This leads to wetting in the Mediterranean and drying in northwestern Europe. The precise mechanisms—possibly involving weakened equatorial convergence or West African monsoon suppression—remain uncertain.

### 3.3. Tropical Hydroclimate Responses and Mechanisms

Tropical hydroclimate reconstructions remain comparatively uncertain due to limited proxy coverage and seasonal resolution. While drought atlases provide valuable regional records, they offer sparse information for equatorial and monsoonal zones (only drought atlases spanning the last millennium have been taken into account here). Consequently, DA products such as LMR and PHYDA are essential for assessing tropical hydroclimatic responses. Despite differences in assimilation strategy and seasonality, both reconstructions show coherent drying in key regions—including the Maritime Continent, equatorial Africa, and Central America—after major tropical eruptions (Tejedor et al. 2021a, He et al. 2026) (**Figure 2**). These dry anomalies are often interpreted as the result of southward displacement of the ITCZ. Hemispheric asymmetries in posteruption cooling—particularly stronger cooling in the NH—reduce northward energy fluxes, shifting the ITCZ southward and weakening NH summer monsoons (see Section 2). This shift suppresses convection in typically rain-rich zones near the equator and alters the tropical Walker circulation, which can become weakened or spatially shifted, reducing moisture convergence over the western Pacific and tropical Americas. Reconstructions and models alike support this mechanism, with evidence of reduced rainfall in South Asia, West Africa, and Central America.

### 3.4. ENSO Response: Diverging Evidence

One of the most debated tropical responses to volcanic eruptions is their influence on ENSO. Several modeling and proxy studies have proposed that large tropical eruptions favor or trigger El Niño–like conditions (e.g., Ohba et al. 2013, Maher et al. 2015, Pausata et al. 2015, Khodri et al. 2017). However, other analyses based on coral proxies and DA products (Dee et al. 2020, Dee & Steiger 2022, Zhu et al. 2022) find inconsistent or statistically weak posteruption Niño 3.4 anomalies. Some reconstructions indicate warming; others show neutral or even La Niña–like conditions (e.g., Zhu et al. 2020). This lack of consensus likely reflects multiple factors, including internal ENSO variability, eruption seasonality, and uncertainties in proxy sensitivity and eruption dating. In addition, methodological differences may play a role. For instance, some studies do not adopt a relative sea-surface temperature (SST) framework—i.e., they examine Niño 3.4 absolute SSTs instead of anomalies relative to broader tropical averages—making it difficult to disentangle ENSO-specific responses from basin-wide radiative cooling. A recent reconstruction of Pacific Ocean sea-level pressure gradient suggests that volcanic eruptions trigger El Niño–like Walker circulation weakening, similar to the response simulated by climate models (Falster et al. 2023). Within these uncertainties, the prevailing view is that volcanic forcing may modulate the probability distribution of ENSO states without reliably triggering a canonical El Niño or La Niña event. A detailed explanation of physical mechanisms is discussed in Section 4.

### 3.5. Persistence of Hydroclimatic Anomalies

The duration of hydroclimatic anomalies varies across datasets. In PHYDA, wetting persists for up to a decade in some regions, such as the Middle East and southern South America. LMR shows prolonged wettening in western North America, potentially reflecting biological memory effects in tree-ring proxies (He et al. 2026). By contrast, model simulations [e.g., Community Earth System Model version 1 Last Millennium Ensemble (CESM1-LME)] generally simulate shorter-lived responses (2–3 years), potentially due to the absence of memory processes or underrepresentation of key feedbacks. Recent efforts to reconcile these differences emphasize the role of proxy-model integration. Lücke et al. (2019) showed that incorporating autoregressive memory into models improves spectral agreement with proxy data. Zhu et al. (2020) demonstrated that model-reconstruction discrepancies in volcanic cooling can be narrowed by comparing seasonal responses at proxy sites and prioritizing high-sensitivity proxies such as MXD. These insights highlight how methodological details—including proxy selection, temporal resolution, and site-specific comparisons—affect the detection and interpretation of forced hydroclimatic signals. Although reconstructions (including DA products) reveal persistent hydroclimatic anomalies, their relationship to the underlying energetic constraints of the climate system remains debated. In theory, postvolcanic cooling reduces net radiative input, leading to large-scale energy imbalances that should be compensated by changes in atmospheric circulation and moisture transport. However, the lack of consistency in ENSO responses across reconstructions complicates this interpretation, suggesting that internal variability, nonlinear dynamics, and regional feedbacks may influence the system's response in ways that are not fully accounted for by energetic theory alone. Bridging the gap between reconstructed persistence and physically based frameworks remains a key challenge for future research.

**Matsuno-Gill-type mechanism:** a dynamical response of the tropical atmosphere to localized heating in which convection generates equatorial Kelvin and Rossby wave patterns; these induce characteristic eastward and westward wind and pressure anomalies, providing a framework for understanding how diabatic heating drives large-scale tropical circulation

## 4. MODELING THE IMPACT OF VOLCANIC ERUPTIONS ON TROPICAL HYDROCLIMATE

Understanding the tropical hydroclimate response to volcanic forcing requires process-based insights from climate models for testing theoretical arguments. In Section 2, we showed how the altered energy balances at the surface and top of the atmosphere can largely induce perturbations that modify large-scale atmospheric circulation and precipitation patterns, with particularly strong sensitivity in the tropics where convection and rainfall are tightly coupled to energy fluxes. Climate models provide a crucial framework to isolate the dynamical and thermodynamical pathways through which volcanic forcing influences tropical temperature, precipitation, and circulation. Thus, in this section we examine how models simulate these processes, including their representation of ITCZ shifts (Section 4.1), monsoon systems (Section 4.2), and interannual ENSO variability (Section 4.3).

### 4.1. ITCZ Shifts

Volcanic eruptions—whether tropical or extratropical—perturb the hydrological cycle, primarily by altering tropical precipitation patterns and ITCZ seasonal migration (Robock 2000, Timmreck et al. 2012, Iles & Hegerl 2014, Kremser et al. 2016). Despite uncertainties in observational records and internal variability, modeling studies consistently link volcanic aerosol forcing to an overall drying within the core of the ITCZ for tropical eruptions, or to shifts in the ITCZ's mean latitude for extratropical eruptions, through changes in the atmospheric energy budget within the year following an event (**Figure 3**).

Interhemispherically asymmetric forcing pushes the ITCZ away from the hemisphere that is cooled. Idealized slab-ocean experiments confirm the theory that the HC and ITCZ respond strongly to forcing latitude (Kang et al. 2020). Climate models consistently show that NH-confined volcanic eruptions induce a southward ITCZ shift, weaken equatorial trade winds, and reduce SST gradients; SH-confined eruptions produce the opposite response (e.g., Pausata et al. 2015, 2020; Colose et al. 2016; Stevenson et al. 2016; Ward et al. 2021) (**Figure 3**). Tropical eruptions with a symmetric aerosol distribution typically cool the NH more than the SH, also driving a southward ITCZ shift (e.g, Ward et al. 2021, D'Agostino & Timmreck 2022) (**Figure 3**).

Tropical eruptions can also alter the land–sea energy balance directly: Volcanically induced cooling is often larger over tropical land (e.g., northern Africa) than over the adjacent ocean. The resulting tropical drying anomalies remain phase locked to the ITCZ's annual migration and sustain a weaker Walker circulation via a Matsuno-Gill-type mechanism (Khodri et al. 2017, Liu et al. 2022, Dogar et al. 2023, Falster et al. 2023, Pausata et al. 2023). Fully coupled last millennium

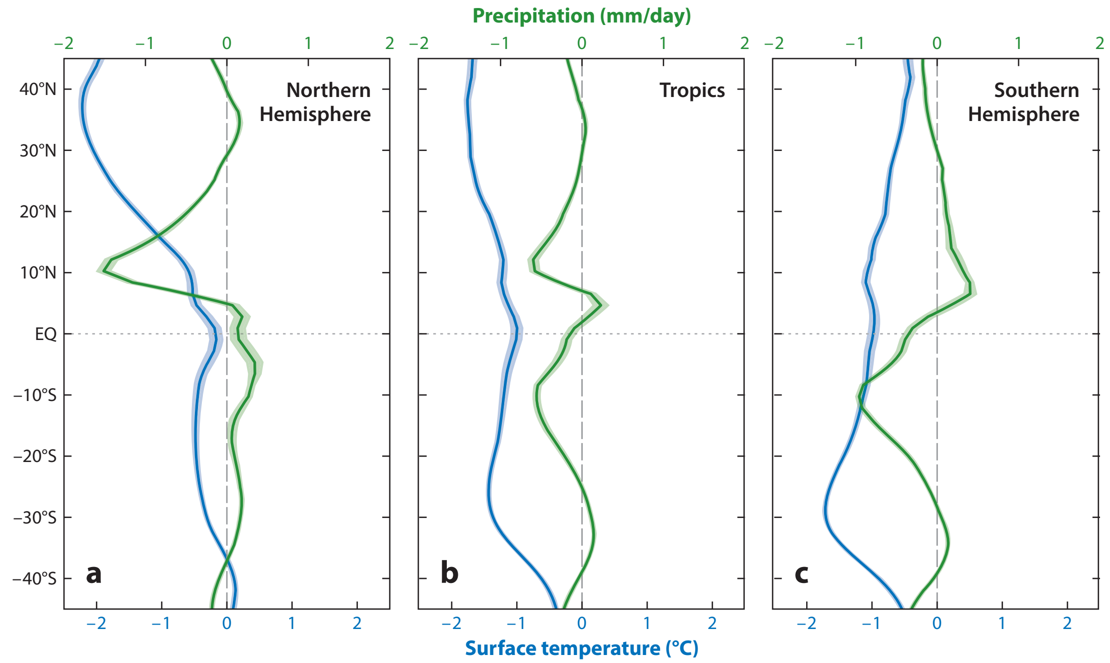


**Figure 3**

Ensemble mean of anomalous zonal mean surface temperature (*blue*) and precipitation (*green*) response to (*a*) Northern Hemisphere, (*b*) tropical, and (*c*) Southern Hemisphere 40-TgS eruptions minus the control run without volcanoes from 100 members of the Max Planck Institute Grand Ensemble Easy Volcanic Aerosol ensemble (MPI-GE EVA-ENS) experiment (Azoulay et al. 2021, Timmreck et al. 2024). The means are computed during the second year from the volcanic eruption (1992), and the shadings are two times the standard error.

Paleoclimate Modeling Intercomparison Project (PMIP) simulations systematically show the ITCZ migrating away from the hemisphere experiencing greater radiative cooling (Colose et al. 2016, Villamayor et al. 2023), as do isotope-enabled CESM runs (Stevenson et al. 2018) and large ensemble simulations with idealized volcanic forcing experiments (**Figure 3**). Other simulations further confirm that NH-constrained aerosol forcing drives a clear southward ITCZ shift, while SH-constrained forcing drives a northward shift (Pausata et al. 2020), emphasizing the energy budget control on tropical precipitation.

## 4.2. Monsoons

Large volcanic eruptions reduce global precipitation, including monsoonal rainfall, by reducing shortwave radiation reaching the surface, lowering evaporation, and stabilizing the atmosphere. Detection and attribution studies, as well as climate model simulations, show that this response results from a combination of thermodynamic effects and circulation changes—particularly ITCZ displacement and a weakening of the HC circulation (e.g., Gillett et al. 2004, Pausata et al. 2015, Liu et al. 2016, Zuo et al. 2018, Dogar & Sato 2019, D'Agostino & Timmreck 2022).

Although regional monsoon responses vary, idealized experiments and large ensemble simulations of the last millennium generally show that eruptions in one hemisphere tend to suppress monsoon rainfall in that hemisphere, while enhancing it in the opposite one, due to the resulting interhemispheric energy imbalance and ITCZ migration (e.g., Liu et al. 2016, Zuo et al. 2018, Dogar & Sato 2019, D'Agostino & Timmreck 2022). In western Africa, eruptions in the NH have been associated with reduced rainfall (Villamayor et al. 2023), while eruptions in the SH tend to produce wetter conditions (Haywood et al. 2013). For the Indian summer monsoon, multiple model simulations consistently indicate a weakening following major eruptions, particularly those located in the tropics or NH (Trenberth & Dai 2007, Liu et al. 2016, Fadnavis et al. 2021). In contrast, the East Asian summer monsoon shows a weaker or mixed response as it is less constrained by the energy framework, due to its sensitivity to both tropical and extratropical circulation dynamics.

On the other hand, the effect of tropical eruptions on monsoons is more uniform, as the volcanic aerosols are transported poleward in both hemispheres and result in a worldwide cooling (Liu et al. 2016), often larger over tropical land than over the adjacent ocean (see **Figure 1**). The result, one year after the eruption, is a general weakening of the monsoonal flow, i.e., dynamic term of the moisture budget and reduced precipitation in the global monsoon domain over land. Idealized experiments with Max Planck Institute Grand Ensemble (MPI-GE) Easy Volcanic Aerosol ensemble (EVA-ENS) have assessed that only a stronger Pinatubo-like eruption (>10 TgS) could result in a significant monsoon decline in every region; otherwise, the response is largely affected by internal variability (D'Agostino & Timmreck 2022).

**Bjerknes feedback:** a self-reinforcing climate process in the tropical Pacific where warmer ocean in the eastern part of the basin weakens the trade winds, which in turn deepen the warm water layer and further increase ocean temperatures, helping to drive El Niño events

## 4.3. Tropical Interannual Variability (ENSO)

As discussed in Section 3, the ENSO response to large tropical eruptions remains a subject of ongoing debate within the proxy-based literature. However, the majority of Model Intercomparison Project on the climatic response to Volcanic forcing (VolMIP) and Coupled Model Intercomparison Project (CMIP) model ensembles are converging, displaying a robust El Niño–like anomaly once direct radiative cooling is accounted for (McGregor et al. 2020, Zanchettin et al. 2022, Dogar et al. 2023).

The strength and sign of this simulated response are sensitive to magnitude, latitude, and timing of the eruption. Large eruptions impose a near-uniform shortwave reduction across the Pacific, producing an immediate surface cooling. As hemispheric gradients develop, the ITCZ shift weakens equatorial trades and activates the Bjerknes feedback over the following months, as demonstrated for the first time in Norwegian Earth System Model simulations by Pausata et al. (2015). Stratospheric aerosol injections confined to the NH drive a southward ITCZ displacement, weakening trade winds and fostering El Niño–like conditions within 6–12 months. SH-confined injections push the ITCZ northward and can weakly favor La Niña–like anomalies (Pausata et al. 2015, 2020; Ward et al. 2021), but these are largely offset by extratropical teleconnections that themselves promote El Niño tendencies irrespective of eruption latitude (see Pausata et al. 2020) (**Figure 4**). When eruptions produce pronounced cooling of tropical northern Africa—whether via NH-confined or symmetrically tropical aerosol distributions—this land cooling generates westerly wind anomalies over the western Pacific that further favor El Niño–like anomalies (Khodri et al. 2017, Pausata et al. 2023). In strictly tropical eruptions, faster NH land cooling again skews the response toward El Niño–like conditions (Ward et al. 2021). Other factors revealed by climate simulations include eruption timing within the seasonal cycle (Predybaylo et al. 2020), background climate state (Pausata et al. 2016, Zanchettin et al. 2022), model ENSO biases (Chen & Jin 2020, Chen et al. 2021), and ensemble size (Pausata et al. 2015, Maher et al. 2019), all of which modulate the ENSO response.

# 5. DISCUSSION AND FUTURE OUTLOOK

This review synthesizes responses of tropical hydroclimate—including tropical overturning circulation, the ITCZ, monsoons, and ENSO—to tropical and extratropical volcanic eruptions, interpreted through the integrative lens of the energy framework discussed in Section 2. The

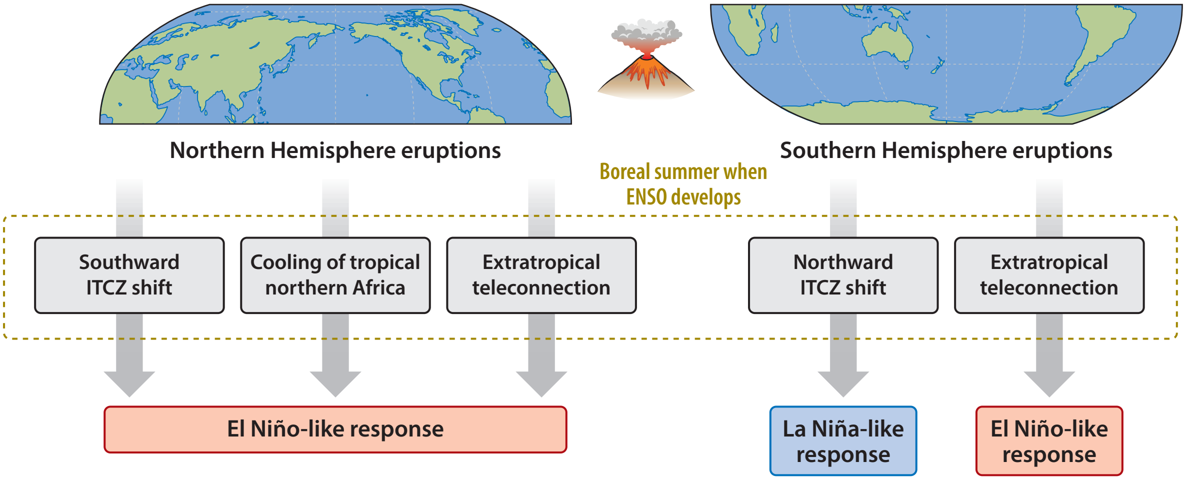


**Figure 4**

Schematic of ENSO-like responses to Northern Hemisphere and Southern Hemisphere eruptions. Abbreviations: ENSO, El Niño–Southern Oscillation; ITCZ, Intertropical Convergence Zone. Figure adapted from Pausata et al. (2020).



rationale for foregrounding the energy budget lies in its capability to elucidate the physical controls on tropical precipitation. The framework provides a coherent basis for interpreting observed and reconstructed posteruption anomalies and constraining projections of hydroclimate responses to future explosive volcanism and associated uncertainties. In this view, the position of the ITCZ and the intensity of tropical overturning circulation are governed by the energetics of the climate system, which has to balance hemispheric asymmetries in radiative forcing. As shown by modeling experiments, and to some extent by reconstructions and observations, volcanic eruptions disrupt this balance in distinct ways primarily depending on their latitude: Tropical eruptions induce a hemispherically near-symmetric reduction in incoming solar radiation, generally weakening the tropical energy flux and reducing rainfall across the whole tropical band; in contrast, extratropical eruptions—especially if the forcing is confined to one hemisphere—generate strong interhemispheric energy imbalances that drive a cross-equatorial AET and a corresponding shift of the ITCZ away from the perturbed hemisphere. This energetically consistent response helps explain key precipitation and temperature patterns in both reconstructed and simulated hydroclimate anomalies following explosive eruptions.

Regarding specific aspects of the tropical hydroclimate response to volcanic forcing, our review highlights the following major recent advancements in understanding and remaining critical gaps of knowledge, which we address by providing recommendations for future research.

Idealized model simulations and past millennium experiments confirm theoretical insights that the ITCZ tends to move away from the hemisphere experiencing stronger volcanic forcing. However, the ITCZ response intertwines with the ENSO response, and nowadays the use of a large ensemble simulation approach appears necessary to disentangle the effects on the ITCZ of direct radiative asymmetries from other dynamical responses of the tropical coupled ocean–atmosphere system. Such an ensemble approach will be an integrative part of the protocol experiments now planned in the next PMIP phase 5 (PMIP5)/past2k initiative.

Regarding monsoons, despite regional differences in sensitivity to volcanic eruption diversity, the simulated responses to volcanic forcing broadly follow the energy framework, but with a strong dependency on the latitudinal position of the eruption. NH extratropical eruptions shift the ITCZ southward, weakening NH monsoons relative to their climatological means, and vice versa. In particular, the Indian summer monsoon shows consistent posteruption weakening, and northern Africa experiences widespread droughts in the Sahel region, while the East Asian summer monsoon response is muted or even reversed due to compensating dynamical effects, often tied to El Niño–like teleconnections. Tropical eruptions, on the other hand, result in worldwide cooling and a uniform weakening of tropical overturning and reduced monsoonal precipitation in both hemispheres, with a peak during the second year after the eruption. Still, in the case of tropical eruptions, the NH cools more than the SH due to large continental masses, and this induces anomalous southward AET that drives the ITCZ equatorward from its climatological position—resembling the response to NH extratropical eruptions. Observations after El Chichón and Pinatubo support these patterns, showing weakened monsoons and equatorward ITCZ shifts lasting up to two years.

**Internal variability (in reconstructions):** can be estimated using a bootstrap superposed epoch analysis, a statistical method to test whether climate changes after volcanic eruptions are unusual; works by creating many fake eruptions at random years in the record, building an expected range of natural variability; the real eruption signals are then compared to this range, and only changes outside it are considered significant

Most of the results we have reported in this review are relative to the tropical mean hydroclimate conditions during the second year after the eruption (>12 months), and the energy framework perfectly describes tropical hydroclimate changes during this period. Few studies have analyzed transient behaviors and have reported few discrepancies from the energetic arguments described here, despite uncertainties regarding the relative contributions of ocean and atmosphere to the total meridional heat transport. For example, Erez & Adam (2021) reported the unexpected predominance of the oceanic energy transport on the atmospheric counterpart during the first posteruption year, with the EFE and ITCZ being decoupled. However, their model setup could not disentangle the relative roles of volcanic forcing and ENSO phases: By affecting the atmospheric and oceanic energy fluxes (as well as surface conditions), the ENSO-like variations modulate the transient ITCZ response and contribute to the contrasting responses by the various energy transport elements. In order to disentangle the effects of volcanic forcing and ENSO changes on tropical hydroclimate, a strong enough volcanic forcing and large ensemble simulations are necessary.

Concerning ENSO itself, climate models increasingly agree that large tropical eruptions tend to trigger an El Niño–like response within the first year, once the direct radiative cooling is accounted for. This tendency arises because aerosol-induced surface cooling and evolving hemispheric temperature gradients drive the ITCZ southward, weaken equatorial trade winds, and activate the Bjerknes feedback. Eruptions confined to the NH reinforce these El Niño–like anomalies, while SH-confined injections can briefly favor La Niña–like conditions, although these are often offset by extratropical teleconnections that also promote eastern Pacific warming. For tropical events with symmetric interhemispheric forcing, the tendency toward posteruption El Niño–like conditions is rooted in the rapid cooling of northern African land areas that trigger westerly wind anomalies over the western equatorial Pacific via a Matsuno-Gill-like mechanism. Importantly, eruption magnitude, latitude, seasonal timing, background climate state, and model characteristics (e.g., ENSO biases, ensemble size) all modulate the strength and sign of the ENSO response. Moving forward, adopting standardized volcanic forcing protocols (VolMIP) and larger, isotope-enabled ensembles directly compared against coral and tree-ring records—currently the most reliable proxies of ENSO—appears to be essential to constrain the full range of volcanic impacts on Earth's dominant mode of interannual variability.

Paleoclimate reconstructions remain essential for assessing the tropical hydroclimate response to volcanic eruptions. Temperature signals are robust and consistent across reconstruction types over land, underscoring volcanic forcing as a dominant driver of short-term widespread cooling in the tropics. In contrast, reconstructed precipitation responses in the tropics are more spatially variable and sensitive to regional dynamics, internal variability, and methodological choices. Despite this uncertainty, certain hydroclimatic patterns, consistent with energetic arguments, emerge with greater confidence—particularly in regions with dense coverage of high-resolution proxy records and coherent signals across multiple reconstruction methods. More specifically regarding ENSO, while there is a consensus on simulated ENSO responses, the SST-based Niño index in reconstructions shows contrasting results, with some records indicating weak El Niño or even La Niña in the first posteruption year. In fact, no significant ENSO response has recently been found in corals and DA products probably due to the difficulty in detecting the relative warming respective to the overall tropical cooling. However, reconstructed tropical Pacific zonal sea-level pressure anomalies point to a significant weakening of the Walker circulation the year after a volcanic eruption, which is consistent with an El Niño–like event. **Table 1** summarizes the findings in model simulations and reconstructions and their agreement with theoretical expectations. In spite of the qualitative agreement on tropical hydroclimate response to volcanic eruptions, there are still large uncertainties on both the quantification of the emission strength and the overall climate response, especially at the regional scale.

Uncertainty in simulating volcanic impacts on climate largely stems from difficulties in quantifying radiative forcing. Estimates are typically based on satellite observations of sulfur emissions combined with global aerosol models, but large discrepancies exist among them due to differences in transport, chemistry, and eruption parameters (height, duration, strength) (Quaglia et al. 2023). The SPARC (Stratosphere-troposphere Processes And their Role in Climate) SSiRC (Stratospheric Sulphur and its Role in Climate) VolRes (Volcano response plan after the next major eruption) initiative aims to provide near-real-time emission estimates to reduce these uncertainties (Vernier et al. 2024). Most climate simulations, however, still rely on idealized forcing prescriptions, which capture broad mechanisms but are difficult to compare with observations and are less reliable for mid- and high-latitude eruptions. For instance, Marshall et al. (2025) found notable differences in surface temperature responses between $SO_2$-emissions-driven and prescribed-forcing simulations of the last millennium, underscoring the importance of the magnitude, latitude, and season of eruptions. Yet, accurately reconstructing eruption season and height from ice-core records remains essential but challenging without precise eruption locations, while additional uncertainties arise from ice-core measurement errors and transfer functions used to infer sulfur emissions (Toohey & Sigl 2017, Sigl et al. 2022).

Then, uncertainties in the climatic response inflate volcanic forcing uncertainty due to limitations in model physics and in constraints in initial conditions. Analysis of simulated tropical precipitation over three generations of CMIP models (Fiedler et al. 2020) has revealed structural deficiencies in coarse-resolution global climate models. This suggests that current coupled climate models with parameterized convection generally poorly simulate changes in tropical precipitation, whether due to anthropogenic or natural forcing. Fortunately, global storm-resolving models (SRMs) with a horizontal resolution of a few kilometers now offer an exciting new approach that would overcome many of these limitations. At these scales, many physical processes, such as atmospheric convection, can be explicitly resolved, thereby improving the reliability of simulated dynamics, including tropical hydroclimatic response to volcanic eruptions. Studying the impact of large volcanic eruptions on tropical hydroclimate using global SRMs could help us to better understand the contribution of the unresolved part of the variability spectrum in low-resolution climate runs, and how weather patterns and local orography affect simulated changes in tropical rainfall. However, SRMs are computationally expensive and may not allow for the large number of realizations that are required to reliably constrain posteruption responses under forcing and initial condition uncertainties. If feasible, utilizing available model hierarchy by combining SRM experiments with CMIP-class model ensembles may help to reconcile some existing discrepancies between model simulations and proxy reconstructions in the aftermath of a volcanic eruption.

**Table 1 Summary of mean hydroclimate response to volcanic eruptions during the second year after the eruptions**

| Response | Theory | Reconstruction | Model simulation | Open question |
|---|---|---|---|---|
| Temperature | Differential cooling in the hemisphere with volcanic eruption or global cooling for tropical eruptions | Broad agreement on hemispheric and global cooling posteruption; peak response ~1–2 years after event | Intermodel agreement for consistent forcing | Regional patterns and the influence of initial conditions in shaping the posteruption temperature response are not fully understood. |
| Hadley circulation/ITCZ | Hemispheric asymmetry in radiative forcing causes interhemispheric energy imbalance → ITCZ shift toward the warmer hemisphere; Hadley circulation weakening | Southward ITCZ shift inferred in drought atlases and data assimilation products following tropical eruptions, particularly those with higher aerosol loading in the NH, which results in drying across regions such as West Africa, Central America, and equatorial Asia | Models simulate ITCZ shifts with NH eruptions and weakening of tropical overturning circulation | The magnitude and timing of ITCZ shifts are still poorly constrained (in simulations and reconstructions). The proxy coverage in tropical regions remains sparse, limiting the potential validation of model results. |
| Monsoon/ atmospheric circulation | Thermodynamic and dynamic suppression of the monsoon for tropical eruptions; weakening in the cooler hemisphere and vice versa | Weakening of South Asian, West African, and American monsoons | Reduced precipitation in the hemisphere where the eruption occurs; general weakening and drying for tropical eruptions | Large regional differences arising from the superposition of internal variability, local SST feedback, and moist static energy gradients make the monsoon response to volcanic eruptions very different from model to model. The lack of high-resolution seasonal reconstructions complicates model-data comparative assessments. |
| ENSO | Volcanic cooling weakens the Walker circulation and enhances air–sea interactions that potentially trigger westerly wind bursts in the western Pacific, a key driver of El Niño; however, the ENSO response also critically depends on the spatial structure of the forcing and hence on the ITCZ response | Contrasting proxy responses (coral, tree rings, data assimilation): some show posteruption El Niño–like patterns; others show neutral or La Niña–like patterns | Consistent tendency of an initial posteruption El Niño when diagnosed with relative SST to exclude the direct radiative cooling in the tropics, but triggered with a variety of mechanisms; later responses of ENSO are less consistent across models | Is the ENSO response deterministic, stochastic, or state dependent? Uncertainty remains due to the role of internal variability, eruption seasonality, preeruption ENSO phase, and dating imprecision. Linear versus nonlinear responses are still debated. |

Abbreviations: ENSO, El Niño–Southern Oscillation; ITCZ, Intertropical Convergence Zone; NH, Northern Hemisphere; SST, sea-surface temperature.

Dedicated model intercomparison experiments—with well-defined protocols and common evaluation metrics—may also offer a path forward. Standardized forcing protocols (e.g., VolMIP) and larger, isotope-enabled ensembles sampling the wide range of the past millennium internal variability (e.g., PMIP5/past2k) compared directly against coral and tree-ring records will be crucial to fully constrain how volcanic forcing contributes to ENSO variability. Idealized volcanic forcing experiments with interhemispheric forcing asymmetries were recently advocated in an intercomparison study (Zanchettin et al. 2022) whose output would allow fully exploiting the energy framework proposed here. Intercomparison initiatives have demonstrated how close cooperation between scientists from different communities—including modeling, DA, proxy reconstruction, and observational science—is essential for framing relevant scientific questions and improving our understanding of volcanic impacts on climate. We advocate that the international scientific community continues fostering such initiatives.

On the proxy-based reconstruction side, future progress will depend on expanding and densifying proxy networks in data-sparse tropical regions, particularly in tropical Africa and tropical South America. Improved constraints on eruption timing and magnitude are also essential to reduce uncertainties in event-aligned composites. Enhanced integration between proxy-based reconstructions and DA frameworks over the past 2,000 years can help isolate forced signals by testing the climatic response when assimilating selected proxies (e.g., only high-resolution tree rings, corals, or isotopes). For instance, targeted DA experiments can shed light on the sensitivity of different proxy types to ENSO-related postvolcanic variability. This would require uncertainty quantification analysis including that related to the model prior from standardized large ensemble protocols that will be developed as part of the next PMIP5/past2k initiative. Moreover, the use of forward proxy modeling—such as integrating mechanistic models of proxy formation (e.g., water isotope or coral growth models) into assimilation frameworks—would improve physical consistency between models and proxies. Isotope-enabled simulations are increasingly being used for this purpose, and ongoing development of isotope-enabled paleoclimate DA systems holds promise for better capturing hydroclimatic responses across the tropics. High-resolution, pantropical coral-based SST reconstructions extending into the last millennium (Dee & Steiger 2022, D'Olivo et al. 2024) will be key for resolving ENSO dynamics, as reliable estimates of Niño 3.4 variability require not just local SSTs but also the basin-wide SST gradients that define ENSO-relative anomaly patterns. Such expanded coverage will allow for more robust assessment of the tropical Pacific response to volcanic forcing.

## DISCLOSURE STATEMENT

The authors are not aware of any affiliations, memberships, funding, or financial holdings that might be perceived as affecting the objectivity of this review.

## AUTHOR CONTRIBUTIONS

R.D. conceptualized the framing, wrote Section 2, and prepared **Figure 1**. M.K. provided inputs in Sections 3 and 4. S.-W.F. contributed to the writing of Section 4 and prepared **Figures 3** and **4**. F.S.R.P. contributed to the writing of Section 4. E.T. wrote Section 3 and prepared **Figure 2**. C.T. and D.Z. wrote Section 1. All authors reviewed and commented on earlier drafts and contributed to Section 5 and to the discussions throughout the development of the manuscript. All authors approved the final version.

## ACKNOWLEDGMENTS

M.K. acknowledges financial support from government funding managed by the French National Research Agency under France 2030, reference ANR-25-EXTR-0001, from the Institut

Pierre-Simon Laplace Climate Graduate School École Universitaire de Recherche, and from Très Grand Centre de Calcul du CEA under the allocations A0150113826, A0160113826, and A0170113826 provided by Grand équipement national de calcul intensif. F.S.R.P. acknowledges financial support from the Natural Sciences and Engineering Research Council of Canada (grant RGPIN-2018-04981). E.T. received funding from the Comunidad de Madrid program Atracción Talento "César Nombela" grant 2023-T1/ECO-29118. C.T. acknowledges funding by German national funding agency research unit FOR 2820: Revisiting the Volcanic Impact on Atmosphere and Climate - Preparations for the Next Big Volcanic Eruption (VolImpact, project 398006378). D.Z. was supported by the DEMETRA research line within the ROSE (Reinforcement of the Observational Systems of the Earth) infrastructural project of INGV (OB.FU.: 1215.010), funded by the Italian Ministry of University and Research. The authors acknowledge comments on an earlier draft provided by Andrew Schurer and Kira Rehfeld. R.D. acknowledges Karin Meier-Fleischer at Deutsches Klimarechenzentrum, Hamburg, for technical support in producing **Figure 1**.



## LITERATURE CITED

Adam O, Bischoff T, Schneider T. 2016. Seasonal and interannual variations of the energy flux equator and ITCZ. Part I: zonally averaged ITCZ position. *J. Clim.* 29(9):3219–30

Alfaro-Sánchez R, Nguyen H, Klesse S, Hudson A, Belmecheri S, et al. 2018. Climatic and volcanic forcing of tropical belt northern boundary over the past 800 years. *Nat. Geosci.* 11(12):933–38

Anchukaitis KJ, Wilson R, Briffa KR, Büntgen U, Cook ER, et al. 2017. Last millennium Northern Hemisphere summer temperatures from tree rings: part II, spatially resolved reconstructions. *Quat. Sci. Rev.* 163:1–22

Atwood AR, Donohoe A, Battisti DS, Liu X, Pausata FS. 2020. Robust longitudinally variable responses of the ITCZ to a myriad of climate forcings. *Geophys. Res. Lett.* 47(17):e2020GL088833

Aubry TJ, Toohey M, Schmidt A, Kovilakam M, Sigl M, et al. 2025. Historical stratospheric aerosol optical properties and volcanic sulfur emissions for CMIP7 Fast Track. Dataset and preliminary documentation. Presented at EGU General Assembly 2025, April 27 to May 2

Azoulay A, Schmidt H, Timmreck C. 2021. The Arctic polar vortex response to volcanic forcing of different strengths. *J. Geophys. Res. Atmos.* 126(11):e2020JD034450

Bilbao R, Ortega P, Swingedouw D, Hermanson L, Athanasiadis P, et al. 2024. Impact of volcanic eruptions on CMIP6 decadal predictions: a multi-model analysis. *Earth Syst. Dyn.* 15:501–25

Bischoff T, Schneider T. 2014. Energetic constraints on the position of the intertropical convergence zone. *J. Clim.* 27(13):4937–51

Brönnimann S, Franke J, Nussbaumer SU, Zumbühl HJ, Steiner D, et al. 2019. Last phase of the Little Ice Age forced by volcanic eruptions. *Nat. Geosci.* 12:650–56

Büntgen U, Di Cosmo N, Esper J, Frachetti M, Khalidi L, et al. 2026. Volcanoes, climate, and society. *Annu. Rev. Earth Planet. Sci.* 54:23–53

Chen HC, Jin FF. 2020. Fundamental behavior of ENSO phase locking. *J. Clim.* 33(5):1953–68

Chen HC, Jin FF, Zhao S, Wittenberg AT, Xie S. 2021. ENSO dynamics in the E3SM-1-0, CESM2, and GFDL-CM4 climate models. *J. Clim.* 34(23):9365–84

Chylek P, Folland C, Klett JD, Dubey MK. 2020. CMIP5 climate models overestimate cooling by volcanic aerosols. *Geophys. Res. Lett.* 47:e2020GL087047

Colose CM, LeGrande AN, Vuille M. 2016. Hemispherically asymmetric volcanic forcing of tropical hydroclimate during the last millennium. *Earth Syst. Dyn.* 7(3):681–96

Cook BI, Cook ER, Anchukaitis KJ, Singh D. 2024. Characterizing the 2010 Russian heat wave–Pakistan flood concurrent extreme over the last millennium using the Great Eurasian Drought Atlas. *J. Clim.* 37:4389–401

Cook ER, Seager R, Heim RR Jr., Vose RS, Herweijer C, Woodhouse C. 2010. Megadroughts in North America: placing IPCC projections of hydroclimatic change in a long-term palaeoclimate context. *J. Quat. Sci.* 25:48–61

D'Agostino R, Bader J, Bordoni S, Ferreira D, Jungclaus J. 2019. Northern Hemisphere monsoon response to mid-Holocene orbital forcing and greenhouse gas-induced global warming. *Geophys. Res. Lett.* 46(3):1591–601

D'Agostino R, Brown JR, Moise A, Nguyen H, Silva Dias PL, Jungclaus J. 2020. Contrasting Southern Hemisphere monsoon response: midHolocene orbital forcing versus future greenhouse gas–induced global warming. *J. Clim.* 33(22):9595–613

D'Agostino R, Timmreck C. 2022. Sensitivity of regional monsoons to idealised equatorial volcanic eruption of different sulfur emission strengths. *Environ. Res. Lett.* 17(5):054001

Dee SG, Cobb KM, Emile-Geay J, Ault TR, Edwards RL, et al. 2020. No consistent ENSO response to volcanic forcing over the last millennium. *Science* 367(6485):1477–81

Dee SG, Steiger NJ. 2022. ENSO's response to volcanism in a data assimilation-based paleoclimate reconstruction over the Common Era. *Paleoceanogr. Paleoclimatol.* 37:e2021PA004290

Dogar MM. 2018. Impact of tropical volcanic eruptions on Hadley circulation using a high-resolution AGCM. *Curr. Sci.* 114(6):1284–94

Dogar MM, Hermanson L, Scaife AA, Visioni D, Zhao M, et al. 2023. A review of El Niño Southern Oscillation linkage to strong volcanic eruptions and post-volcanic winter warming. *Earth Syst. Environ.* 7(1):15–42

Dogar MM, Sato T. 2019. Regional climate response of Middle Eastern, African, and South Asian monsoon regions to explosive volcanism and ENSO forcing. *J. Geophys. Res. Atmos.* 124(14):7580–98

D'Olivo JP, Zinke J, Goyal R, England MH, Purich A, et al. 2024. Coral Sr/Ca-SST reconstruction from Fiji extending to ∼1370 CE reveals insights into the Interdecadal Pacific Oscillation. *Sci. Adv.* 10(33):eado5107

Douville H, Raghavan K, Renwick J, Allan RP, Arias PA, et al. 2021. Water cycle changes. In *Climate Change 2021: The Physical Science Basis. Contribution of Working Group I to the Sixth Assessment Report of the Intergovernmental Panel on Climate Change*, ed. V Masson-Delmotte, P Zhai, A Pirani, SL Connors, C Péan, et al. Cambridge University Press

Erez M, Adam O. 2021. Energetic constraints on the time-dependent response of the ITCZ to volcanic eruptions. *J. Clim.* 34(24):9989–10006

Eyring V, Gillett N, Achuta Rao K, Barimalala R, Barreiro Parrillo M, et al. 2021. Human influence on the climate system. In *Climate Change 2021: The Physical Science Basis. Contribution of Working Group I to the Sixth Assessment Report of the Intergovernmental Panel on Climate Change*, ed. V Masson-Delmotte, P Zhai, A Pirani, SL Connors, C Péan, et al. Cambridge University Press

Fadnavis S, Müller R, Chakraborty T, Sabin TP, Laakso A, et al. 2021. The role of tropical volcanic eruptions in exacerbating Indian droughts. *Sci. Rep.* 11(1):2714

Falster G, Konecky B, Coats S, Stevenson S. 2023. Forced changes in the Pacific Walker circulation over the past millennium. *Nature* 622(7981):93–100

Fiedler S, Crueger T, D'Agostino R, Peters K, Becker T, et al. 2020. Simulated tropical precipitation assessed across three phases of the Coupled Model Intercomparison Project (CMIP). *Mon. Weather Rev.* 148:3653–80

Geen R, Bordoni S, Battisti DS, Hui K. 2020. Monsoons, ITCZs, and the concept of the global monsoon. *Rev. Geophys.* 58(4):e2020RG000700

Gillett NP, Weaver AJ, Zwiers FW, Wehner MF. 2004. Detection of volcanic influence on global precipitation. *Geophys. Res. Lett.* 31(12):L12217

Haywood JM, Jones A, Bellouin N, Stephenson D. 2013. Asymmetric forcing from stratospheric aerosols impacts Sahelian rainfall. *Nat. Clim. Change* 3(7):660–65

He Z, Tejedor E, Smerdon JE, Vuille M, Polvani LM, et al. 2026. Comparison of global climatic responses to large tropical volcanic eruptions over the last millennium in paleoclimatic reconstructions and model simulations. *J. Clim.* 39:1295–313

Hegerl GC, Black E, Allan RP, Ingram WJ, Polson D, et al. 2015. Challenges in quantifying changes in the global water cycle. *Bull. Am. Meteorol. Soc.* 96:1097–115

Iles CE, Hegerl GC. 2014. The global precipitation response to volcanic eruptions in the CMIP5 models. *Environ. Res. Lett.* 9(10):104012
Iles CE, Hegerl GC. 2015. Systematic change in global patterns of streamflow following volcanic eruptions. *Nat. Geosci.* 8(11):838–42
Iles CE, Hegerl GC, Schurer AP, Zhang X. 2013. The effect of volcanic eruptions on global precipitation. *J. Geophys. Res. Atmos.* 118(16):8770–86
Joseph R, Zeng N. 2011. Seasonally modulated tropical drought induced by volcanic aerosol. *J. Clim.* 24(8):2045–60
Kang SM, Frierson DM, Held IM. 2009. The tropical response to extratropical thermal forcing in an idealized GCM: the importance of radiative feedbacks and convective parameterization. *J. Atmos. Sci.* 66(9):2812–27
Kang SM, Held IM, Frierson DMW, Zhao M. 2008. The response of the ITCZ to extratropical thermal forcing: idealized slab-ocean experiments with a GCM. *J. Clim.* 21(14):3521–32
Kang SM, Xie SP, Shin Y, Kim H, Hwang YT, et al. 2020. Walker circulation response to extratropical radiative forcing. *Sci. Adv.* 6(47):eabd3021
Khodri M, Izumo T, Vialard J, Janicot S, Cassou C, et al. 2017. Tropical explosive volcanic eruptions can trigger El Niño by cooling tropical Africa. *Nat. Commun.* 8(1):778
Kremser S, Thomason LW, von Hobe M, Hermann M, Deshler T, et al. 2016. Stratospheric aerosol—observations, processes, and impact on climate. *Rev. Geophys.* 54:278–335
Lehner F, Schurer AP, Hegerl GC, Deser C, Frölicher TL. 2016. The importance of ENSO phase during volcanic eruptions for detection and attribution. *Geophys. Res. Lett.* 43(6):2851–58
Lionello P, D'Agostino R, Ferreira D, Nguyen H, Singh MS. 2024. The Hadley circulation in a changing climate. *Ann. N. Y. Acad. Sci.* 1534(1):69–93
Liu F, Chai J, Wang B, Liu J, Zhang X, Wang Z. 2016. Global monsoon precipitation responses to large volcanic eruptions. *Sci. Rep.* 6(1):24331
Liu F, Xing C, Chen L, Gao C, Lian T, et al. 2022. Relative roles of land and ocean cooling in triggering an El Niño following tropical volcanic eruptions. *Geophys. Res. Lett.* 49:e2022GL100609
Lücke LJ, Hegerl GC, Schurer AP, Wilson R. 2019. Effects of memory biases on variability of temperature reconstructions. *J. Clim.* 32(24):8713–31
Maher N, England MH, Gupta AS. 2015. Effects of volcanism on tropical variability. *Geophys. Res. Lett.* 42(13):6024–33
Maher N, Milinski S, Suarez-Gutierrez L, Botzet M, Dobrynin M, et al. 2019. The Max Planck Institute Grand Ensemble: enabling the exploration of climate system variability. *J. Adv. Model. Earth Syst.* 11(7):2050–69
Marotzke J, Forster P. 2015. Forcing, feedback and internal variability in global temperature trends. *Nature* 517:565–70
Marshall J, Donohoe A, Ferreira D, McGee D. 2014. The ocean's role in setting the mean position of the Inter-Tropical Convergence Zone. *Clim. Dyn.* 42(7):1967–79
Marshall LR, Maters EC, Schmidt A, Timmreck C, Robock A, Toohey M. 2022. Volcanic effects on climate: recent advances and future avenues. *Bull. Volcanol.* 84(5):54
Marshall LR, Schmidt A, Schurer AP, Abraham NL, Lücke LJ, et al. 2025. Last-millennium volcanic forcing and climate response using $SO_2$ emissions. *Clim. Past* 21:161–84
McGraw Z, Polvani LM. 2024. How volcanic aerosols globally inhibit precipitation. *Geophys. Res. Lett.* 51(13):e2023GL107930
McGregor S, Khodri M, Maher N, Ohba M, Pausata FS, Stevenson S. 2020. The effect of strong volcanic eruptions on ENSO. In *El Niño/Southern Oscillation in a Changing Climate*, ed. MJ McPhaden, A Santoso, W Cai. American Geophysical Union
Neelin JD, Held IM. 1987. Modeling tropical convergence based on the moist static energy budget. *Mon. Weather Rev.* 115(1):3–12
Ohba M, Shiogama H, Yokohata T, Watanabe M. 2013. Impact of strong tropical volcanic eruptions on ENSO simulated in a coupled GCM. *J. Clim.* 26:5169–82
Pausata FS, Grini A, Caballero R, Hannachi A, Seland Ø. 2015. High-latitude volcanic eruptions in the Norwegian Earth System Model: the effect of different initial conditions and of the ensemble size. *Tellus B Chem. Phys. Meteorol.* 67(1):26728

Pausata FS, Karamperidou C, Caballero R, Battisti DS. 2016. ENSO response to high-latitude volcanic eruptions in the Northern Hemisphere: the role of the initial conditions. *Geophys. Res. Lett.* 43(16):8694–702

Pausata FS, Zanchettin D, Karamperidou C, Caballero R, Battisti DS. 2020. ITCZ shift and extratropical teleconnections drive ENSO response to volcanic eruptions. *Sci. Adv.* 6(23):eaaz5006

Pausata FS, Zhao Y, Zanchettin D, Caballero R, Battisti DS. 2023. Revisiting the mechanisms of ENSO response to tropical volcanic eruptions. *Geophys. Res. Lett.* 50(3):e2022GL102183

Predybaylo E, Stenchikov G, Wittenberg AT, Osipov S. 2020. El Nino/Southern Oscillation response to low-latitude volcanic eruptions depends on ocean pre-conditions and eruption timing. *Commun. Earth Environ.* 1(1):12

Quaglia I, Timmreck C, Niemeier U, Visioni D, Pitari G, et al. 2023. Interactive stratospheric aerosol models' response to different amounts and altitudes of $SO_2$ injection during the 1991 Pinatubo eruption. *Atmos. Chem. Phys.* 23(2):921–48

Rao MP, Cook BI, Cook ER, D'Arrigo RD, Krusic PJ, et al. 2017. European and Mediterranean hydroclimate responses to tropical volcanic forcing over the last millennium. *Geophys. Res. Lett.* 44(10):5104–12

Ridley HE, Asmerom Y, Baldini JU, Breitenbach SF, Aquino VV, et al. 2015. Aerosol forcing of the position of the intertropical convergence zone since AD 1550. *Nat. Geosci.* 8(3):195–200

Robock A. 2000. Volcanic eruptions and climate. *Rev. Geophys.* 38(2):191–219

Schneider L, Smerdon JE, Büntgen U, Wilson RJS, Myglan VS, et al. 2015. Revising mid-latitude summer temperatures back to A.D. 600 based on a wood density network. *Geophys. Res. Lett.* 42:4556–62

Schurer AP, Ballinger AP, Friedman AR, Hegerl GC. 2020. Human influence strengthens the contrast between tropical wet and dry regions. *Environ. Res. Lett.* 15(10):104026

Seager R, Naik N, Vecchi GA. 2010. Thermodynamic and dynamic mechanisms for large-scale changes in the hydrological cycle in response to global warming. *J. Clim.* 23(17):4651–68

Sigl M, Toohey M, McConnell JR, Cole-Dai J, Severi M. 2022. Volcanic stratospheric sulfur injections and aerosol optical depth during the Holocene (past 11,500 years) from a bipolar ice core array. *Earth Syst. Sci. Data Discuss.* 14:3167–96

Steiger NJ, Smerdon JE, Cook ER, Cook BI. 2018. A reconstruction of global hydroclimate and dynamical variables over the Common Era. *Sci. Data* 5:180086

Steinman BA, Stansell ND, Mann ME, Cooke CA, Abbott MB, et al. 2022. Interhemispheric antiphasing of neotropical precipitation during the past millennium. *PNAS* 119(17):e2120015119

Stevenson S, Otto-Bliesner B, Fasullo J, Brady E. 2016. "El Niño like" hydroclimate responses to last millennium volcanic eruptions. *J. Clim.* 29(8):2907–21

Stevenson S, Overpeck JT, Fasullo J, Coats S, Parsons L, et al. 2018. Climate variability, volcanic forcing, and last millennium hydroclimate extremes. *J. Clim.* 31(11):4309–27

Stoffel M, Khodri M, Corona C, Guillet S, Poulain V, et al. 2015. Estimates of volcanic-induced cooling in the Northern Hemisphere over the past 1,500 years. *Nat. Geosci.* 8(10):784–88

Tardif R, Hakim GJ, Perkins WA, Horlick KA, Erb MP, et al. 2019. Last Millennium Reanalysis with an expanded proxy database and seasonal proxy modeling. *Clim. Past* 15:1251–73

Tejedor E, Steiger NJ, Smerdon JE, Serrano-Notivoli R, Vuille M. 2021a. Global hydroclimatic response to tropical volcanic eruptions over the last millennium. *PNAS* 118(12):e2019145118

Tejedor E, Steiger NJ, Smerdon JE, Serrano-Notivoli R, Vuille M. 2021b. Global temperature responses to large tropical volcanic eruptions in paleo data assimilation products and climate model simulations over the last millennium. *Paleoceanogr. Paleoclimatol.* 36:e2020PA004128

Timmreck C. 2012. Modeling the climatic effects of volcanic eruptions. *WIREs Clim. Change* 3(6):545–64

Timmreck C, Graf HF, Zanchettin D, Hagemann S, Kleinen T, Krüger K. 2012. Climate response to the Toba super-eruption: regional changes. *Quat. Int.* 258:30–44

Timmreck C, Olonscheck D, Ballinger A, D'Agostino R, Fang SW, et al. 2024. Linearity of the climate response to increasingly strong tropical volcanic eruptions in a large ensemble framework. *J. Clim.* 37:2455–70

Timmreck C, Toohey M, Zanchettin D, Brönnimann S, Lundstad E, Wilson R. 2021. The unidentified eruption of 1809: a climatic cold case. *Clim. Past* 17(4):1455–82

Toohey M, Krüger K, Schmidt H, Timmreck C, Sigl M, et al. 2019. Disproportionately strong climate forcing from extratropical explosive volcanic eruptions. *Nat. Geosci.* 12(2):100–7

Toohey M, Sigl M. 2017. Volcanic stratospheric sulphur injections and aerosol optical depth from 500 BCE to 1900 CE. *Earth Syst. Sci. Data* 9:809–31

Toohey M, Stevens B, Schmidt H, Timmreck C. 2016. Easy Volcanic Aerosol (EVA v1.0): an idealized forcing generator for climate simulations. *Geosci. Model Dev.* 9(11):4049–70

Trenberth KE, Dai A. 2007. Effects of Mount Pinatubo volcanic eruption on the hydrological cycle as an analog of geoengineering. *Geophys. Res. Lett.* 34(15):L15702

Vernier JP, Aubry TJ, Timmreck C, Schmidt A, Clarisse L, et al. 2024. The 2019 Raikoke eruption as a testbed used by the Volcano Response group for rapid assessment of volcanic atmospheric impacts. *Atmos. Chem. Phys.* 24(10):5765–82

Villamayor J, Khodri M, Fang SW, Jungclaus JH, Timmreck C, Zanchettin D. 2023. Sahel droughts induced by large volcanic eruptions over the last millennium in PMIP4/past1000 simulations. *Geophys. Res. Lett.* 50(5):e2022GL101478

Ward B, Pausata FS, Maher N. 2021. The sensitivity of the El Niño–Southern Oscillation to volcanic aerosol spatial distribution in the MPI grand ensemble. *Earth Syst. Dyn.* 12(3):975–96

Winter A, Zanchettin D, Miller T, Kushnir Y, Black D, et al. 2015. Persistent drying in the tropics linked to natural forcing. *Nat. Commun.* 6(1):7627

Zanchettin D, Bothe O, Lehner F, Ortega P, Raible C, Swingedouw D. 2015. Reconciling reconstructed and simulated features of the winter Pacific/North American pattern in the early 19th century. *Clim. Past* 11(6):939–58

Zanchettin D, Khodri M, Timmreck C, Toohey M, Schmidt A, et al. 2016. The Model Intercomparison Project on the climatic response to Volcanic forcing (VolMIP): experimental design and forcing input data for CMIP6. *Geosci. Model Dev.* 9(8):2701–19

Zanchettin D, Timmreck C, Khodri M, Schmidt A, Toohey M, et al. 2022. Effects of forcing differences and initial conditions on inter-model agreement in the VolMIP volc-pinatubo-full experiment. *Geosci. Model Dev.* 15:2265–92

Zhu F, Emile-Geay J, Anchukaitis KJ, Hakim GJ, Wittenberg AT, et al. 2022. A re-appraisal of the ENSO response to volcanism with paleoclimate data assimilation. *Nat. Commun.* 13(1):747

Zhu F, Emile-Geay J, Hakim GJ, King J, Anchukaitis KJ. 2020. Resolving the differences in the simulated and reconstructed temperature response to volcanism. *Geophys. Res. Lett.* 47(8):e2019GL086908

Zuo M, Man W, Zhou T, Guo Z. 2018. Different impacts of northern, tropical, and southern volcanic eruptions on the tropical Pacific SST in the last millennium. *J. Clim.* 31(17):6729–44

Zuo M, Zhou T, Man W. 2019a. Hydroclimate responses over global monsoon regions following volcanic eruptions at different latitudes. *J. Clim.* 32(14):4367–85

Zuo M, Zhou T, Man W. 2019b. Wetter global arid regions driven by volcanic eruptions. *J. Geophys. Res. Atmos.* 124(24):13648–62